Final Report

USGS/NEHRP Grants Program

Seismic Investigation of Historical and Recent Earthquakes of the Mendocino Triple Junction Region

July 30, 2005

External Grant: 03HQGR0086

Investigators:

Aaron A. Velasco, University of Texas at El Paso, Geological Sciences, El Paso, TX 79968; Ph: (915) 747-5101; FAX (915) 747-5073; velasco@geo.utep.edu

Diane I. Doser, University of Texas at El Paso, Geological Sciences, El Paso, TX 79968; Ph: (915) 747-5851; FAX (915) 747-5073; doser@geo.utep.edu

Keywords: Seismology, source characteristics, seismotectonics

Period of Performance: 05/01/2003-5/30/2005

Investigation Undertaken

The goal of our study is to better determine the locations, depths, source processes of historic and recent earthquakes, and develop preliminary attenuation models of the Mendocino Triple Junction (MTJ) region in order to 1) quantify the variability in moment release along important features in the MTJ region since 1906, 2) relate the events to specific tectonic features, 3) quantify differences in apparent stresses between intraplate and interplate events, and 4) analyze attenuation and its impact on strong ground motion in the region. The results and products of this study can be applied directly and indirectly to reduce losses from earthquakes in the U.S. The final outcome of our study will include attenuation models and refining our understanding of expected seismogenic zones, rupture processes and stress release, which may all be used to contribute to new seismic hazards maps for the region. The results will also assist in development of earthquake occurrence models by better quantifying changes in moment release since 1906 and the complex interactions of seismogenic features of the MTJ region, especially in relation to the Cascadia Subduction Zone (CSZ). The techniques developed in this study could also applied to studies of historic seismicity in other portions of the United States.

The study represents a collaborative effort between Dr. Aaron Velasco, with expertise in earthquake location algorithms, digital waveform analysis and studies of MTJ seismicity, Dr. Diane Doser, with expertise in historical seismogram acquisition and modeling, and Dr. Roberto Ortega (now at Centro de Investigación Científica y de Educación Superior Ensenada, Unidad La Paz: CICESE, La Paz), with expertise in attenuation model development.

Results

This project is multi-faceted and we report progress for data collection, relocations, source parameters, and an attenuation analysis. The project began on 05/01/2003, and thus we report on the progress for the 19 months up to 12/01/2004. The focus of our study is on the historical (1915-1976) and recent seismicity of the Mendocino Triple Junction region between 123° and 128° W and 39° and 42.5° N. We rely on teleseismic and regional phase arrival times and waveform data obtained from open data sources. The data will be used for earthquake relocation, source parameter, and attenuation studies. Since the last report, we have made significant progress on modeling smaller earthquakes and have investigated the nature of stress in the region.

Task 1: Data Collection

We have gathered both phase data and waveforms from a variety of sources. The data collection is the now complete for this project. We have based our selection of historic earthquakes on searches of the U.S. significant earthquake catalog available at the NEIC website, a summary of felt earthquakes for the MTJ region (to 1992) compiled by Dengler et al. (1992), and the isoseismal studies of Bakun (2000). Prior to 1915 it is difficult to obtain seismograms of sufficient quality for waveform modeling studies. As the station coverage, especially at regional distances, improved through time, we selected smaller magnitude events for study. We are collecting phase data for our relocation effort, and waveform data for source parameter and attenuation studies (see next sections). We outline below the historic data collection and the recent earthquake data collection.

Historical Event Data

We have collected phase data from International Seismological Survey (ISS) obtained at the Caltech archives for pre-1964 earthquakes. The data will be used our relocation effort (described below). The bulk of our collection thus far is after 1937, and we are in the process of transforming it all to digital form (Table 1), since much of it is in paper form. Upon careful examination of this catalog, we have discovered other events not included in our original proposal (Table 1). Thus, we will have more historical events to study than was originally proposed for our relocation effort.

For a number of seismograph stations (e.g. La Paz, DeBilt, Uccle, Weston), we have obtained copies of seismograms directly through written requests to the observatories. Sparks (1936) and Byerly (1938) published important photographic collections of seismograms for the June 1932 and July 1934 earthquakes, respectively. We also collected data from an important regional seismological archives located at Caltech (Figure 1). Table 1 summarized the events and stations for which we now have analog seismograms. We are in the process of scanning these seismograms and digitizing them using *SeisDig*, an interactive MatLab based digitizing tool, designed to digitize entire seismogram "tif" images with a minimum of user interaction. The Integrative Oceanography Division (IOD) of the Scripps Institution of Oceanography, University of California, San Diego developed the program. We expect to have all waveforms digitized by March 2005.

Table 1: Collected waveform data for historic events.

Date	Time	Lat.	Lon.	M/I[1]	Location	Stations w/Waveforms
05/06/1915	12:09	39.50	-126.50	6.8/V$^+$	MFZ/PC	DBN, PAR
12/31/1915	12:29	41.00	-126.00	6.5/III$^+$	Gorda	API, DBN, PAR
07/15/1918	00:23	41.00	-125.00	6.5/VI$^+$	Gorda	API, DBN, LPZ, PAR
01/31/1922	13:17	41.00	-125.50	7.3/VI$^+$	Gorda	API, DMN, LPZ, PAR
01/22/1923	09:04	40.50	-124.50	7.2/VIII$^+$	Gorda	DBN, LPZ
06/06/1932	08:44	40.75	-124.50	6.4	NA	CSC, DBN, LPZ, PAR, PAS, SIT, TUC, UKI, WEL
07/06/1934	22:48	41.22	-125.27	6.5/I$^+$	Gorda	API, CSC, DBN, HON, LPZ, PAR, PAS, SIT, SJP, UKI, WEL
02/07/1937*	04:41	40.40	-125.10	V	Gorda	-
03/26/1937*	29:09	40.30	-126.60	-	MFZ	-
04/22/1937*	09:46	40.90	-125.50	-	Gorda	-
05/06/1937*	14:46	40.40	-125.10	-	Gorda	-
09/12/1938*	06:10	40.40	-125.10	VI	Gorda	-
02/13/1940*	23:52	40.50	-123.50	-	NA	-
12/20/1940*	23:40	39.50	-125.00	VI	MFZ/PC	-
02/09/1941	09:44	40.50	-125.25	6.6/VI$^+$	Gorda	API, DBN, LPZ, PAR, WEL
02/11/1941*	05:50	40.40	-125.10	-	Gorda	-
05/13/1941	16:01	40.30	-126.40	6.0/V$^+$	MFZ	DBN
06/09/1941*	06:17	42.50	-126.30	-	Gorda	-
06/09/1941*	08:43	42.50	-126.30	-	Gorda	-
10/03/1941	16:13	40.40	-124.80	6.4/VII$^+$	Gorda	API, DBN, LPZ
05/19/1945	15:07	40.25	-126.50	6.2/V$^+$	MFZ	-
03/24/1949	20:56	41.30	-126.00	5.9/III$^+$	MFZ	-
10/08/1951	04:10	40.28	-124.80	5.8/VII	MFZ	TUC, PAS, UKI
11/25/1954	11:16	40.27	-125.63	6.1/V	MFZ	-
12/21/1954	19:56	40.78	-124.17	6.5/VII	NA	CHR, COL, CSC, HON, LPZ, MAT, PAS, TUC, WEL
10/11/1956	16:48	40.67	-125.77	6.0/V	Gorda	-
07/24/1959	01:23	41.13	-125.30	5.8/IV	Gorda	MAT
06/06/1960	01:17	40.86	-124.60	5.7/VI	Gorda	-
08/09/1960	07:39	40.47	-126.62	6.2/V	MFZ	-
04/29/1961*	09:19	40.76	-127.42	-	Gorda	-
05/04/1961*	02:17	40.82	-127.46	-	Gorda	-
05/14/1961*	19:31	40.62	-127.44	-	Gorda	-
08/23/1962	19:29	41.84	-124.39	5.6/VI	Gorda	
121067	1206	40.50	-124.60	5.8/VI	Gorda	

062668	0142	40.29	-124.67	5.9/VII	MFZ
030172	0928	40.50	-125.20	5.9/V	Gorda
060775	0846	40.54	-124.29	5.7/VII	NA?

[1]M/I: Magnitude or intensity; MFZ=Mendocino fault zone, NA=North American plate; PC=Pacific plate
*Events not previously identified and discovered with phase data.
Location from historical U.S. catalog of NEIC
+Maximum intensity from Dengler et al. (1992) or NEIC database

Recent Events

For recent events, we have collected phase data for all events in the region that have occurred since 1990 from the USGS Earthquake Data Reports (EDR). We are supplementing this information with phase data from the Northern California Seismic Network (NCSN). We will supplement this information with travel time picks obtained for digital data that we have collected (Table 2).

We have collected waveform data for 151 events (Figure 1; Table 2), significantly expanding the collection that we had originally proposed. Waveform data for stations of the Berkley Digital Seismic Network (BDSN) where also download from the NCSN. We also obtained data for global network stations from the Incorporated Research Institutions for Seismology (IRIS). Current systems make this effort fairly trivial, and we have all of the waveforms needed for this project. All data was recovered in Standard for the Exchange of Earthquake Data (SEED) format, and have been converted to Seismic Analysis Code (SAC) format. However, we will be building a Center for Seismic Studies (CSS) style database from the data collected for our relocation effort. The SAC files are now being utilized for our attenuation analysis (discussed below).

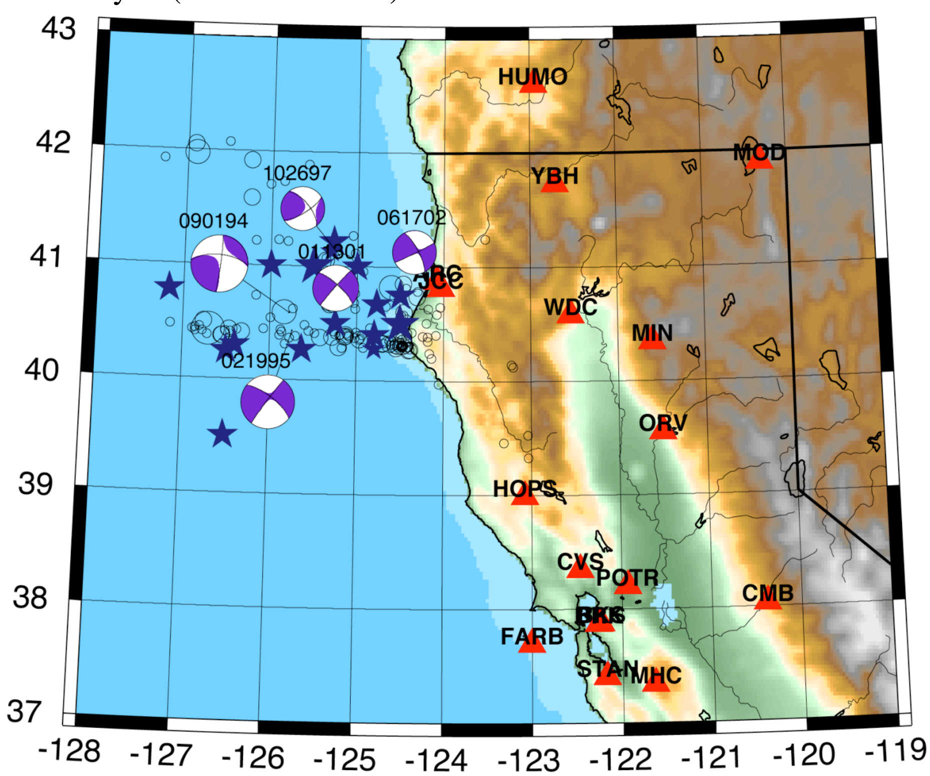

Figure 1: Map showing the locations of historic (blue stars) and recent (open circles) events for which we have collected data at NCSN and other stations (red diamonds). Calibration events for source inversions are given by the CMT solutions (purple focal mechanisms).

Table 2: Collected waveform data for recent events.

Date	Time	Lat	Lon	Depth	Mag	Magt[1]	SRC[2]	CE
1992/06/05	21:46:40.83	40.2878	-124.5408	5.00	4.71	Md	NCSN	
1993/07/27	21:17:21.38	40.3077	-124.4662	8.50	4.03	Md	NCSN	
1993/10/23	18:45:51.05	40.5042	-126.7582	5.11	4.83	Md	NCSN	
1994/02/21	13:40:06.35	40.4022	-125.1843	0.16	3.94	Md	NCSN	
1994/03/02	10:21:44.00	40.6338	-125.2902	7.19	3.51	Md	NCSN	
1994/03/13	16:59:03.91	40.3610	-124.9663	12.53	4.37	Md	NCSN	
1994/05/09	14:14:41.00	42.0490	-126.9120	10.0	4.10	MB	NEIC	
1994/05/24	20:11:38.59	40.9597	-124.9300	4.37	3.16	Md	NCSN	
1994/06/19	10:39:32.85	40.3543	-124.4655	19.25	4.67	Md	NCSN	
1994/07/02	13:43:27.54	40.2997	-124.3995	8.67	3.66	Md	NCSN	
1994/09/01	15:15:44.09	40.4335	-126.7095	5.74	6.13	Mlg	NCSN	*
1994/10/14	00:57:25.43	40.3242	-124.6202	19.33	4.11	Md	NCSN	
1994/11/13	07:53:51.53	40.3983	-125.0922	0.04	3.54	Md	NCSN	
1994/12/26	14:10:29.17	40.7383	-124.3047	23.46	4.92	Mlg	NCSN	
1995/02/19	04:03:14.27	40.5903	-125.8338	5.34	5.75	Mlg	NCSN	*
1995/12/24	07:41:31.00	41.9698	-126.8985	10.0	5.30	MB	ISCCD	
1996/07/24	20:15:41.22	41.9172	-126.2530	2.52	4.90	Md	NCSN	
1996/09/04	10:18:21.79	41.9167	-127.2742	5.00	3.60	Md	NCSN	
1996/09/06	20:42:29.53	40.4142	-126.3200	3.14	4.44	Md	NCSN	
1996/09/27	13:44:44.85	40.4738	-127.1457	24.02	3.69	Md	NCSN	
1997/01/22	07:17:16.75	40.2728	-124.3880	23.64	4.85	Md	NCSN	
1997/06/07	19:39:59.02	40.4323	-126.4663	5.77	4.43	Md	NCSN	
1997/09/21	12:36:27.58	41.5885	-126.2430	3.17	4.31	Md	NCSN	
1997/10/04	10:57:34.34	41.0505	-125.3622	9.88	4.60	Md	NCSN	
1997/10/06	12:00:23.82	41.0713	-125.3665	5.00	3.82	Md	NCSN	
1997/10/26	10:44:08.16	41.0020	-125.1698	5.16	5.24	ML	NCSN	*
1997/12/15	22:42:42.11	40.3157	-124.5533	21.59	4.09	ML	NCSN	
1998-03-23	02:28:10.00	43.4471	-127.0971	10	4.90	MB	ISCCD	
1998/11/27	00:43:48.93	40.6628	-125.3168	5.28	4.86	Md	NCSN	
1999/07/24	00:38:41.21	40.3858	-125.1222	6.61	4.12	Md	NCSN	
1999/11/22	05:38:04.84	40.4005	-125.1262	6.81	4.22	Md	NCSN	
1999/12/26	19:41:53.10	40.2705	-124.4008	23.31	4.19	ML	NCSN	
2000/01/08	02:17:28.31	40.3777	-126.5475	4.99	4.81	Md	NCSN	
2000/02/02	23:14:32.55	40.5105	-124.4533	24.23	3.45	Md	NCSN	
2000/03/16	15:19:55.81	40.3803	-125.2807	5.00	4.76	Md	NCSN	
2000/05/08	09:12:34.47	40.3275	-124.6942	4.00	4.11	ML	NCSN	
2000/08/13	18:17:48.75	40.3657	-124.4728	18.23	3.91	ML	NCSN	
2000/08/21	04:45:13.51	39.3308	-123.0315	13.36	3.73	ML	NCSN	
2000/09/22	10:50:27.20	40.8527	-124.4627	13.24	4.38	ML	NCSN	
2000/10/25	16:48:19.27	40.4122	-125.4813	5.10	3.32	Md	NCSN	
2000/12/27	13:15:11.18	40.4647	-124.4653	28.74	3.96	ML	NCSN	
2001/01/05	15:46:52.50	40.3495	-124.6170	23.85	3.37	ML	NCSN	
2001/01/06	18:09:59.98	40.3818	-126.7205	18.53	3.17	Md	NCSN	
2001/01/11	18:10:40.84	40.6337	-124.1790	23.11	3.95	ML	NCSN	
2001/01/13	13:08:42.32	40.7398	-125.2847	5.60	5.19	ML	NCSN	*
2001/01/22	23:41:14.88	40.4263	-125.5515	23.39	3.05	Md	NCSN	
2001/02/01	06:19:38.93	40.4167	-124.4110	28.32	3.35	ML	NCSN	
2001/02/07	19:19:01.94	40.5760	-124.4627	22.80	3.22	ML	NCSN	
2001/02/07	21:08:43.43	40.5725	-124.4820	23.24	3.25	ML	NCSN	
2001/02/16	17:37:36.33	40.3653	-125.7735	6.41	3.10	Md	NCSN	
2001/02/20	18:51:20.19	40.2907	-124.9200	7.57	3.45	Md	NCSN	
2001/02/22	08:44:57.68	40.3833	-125.7058	2.62	3.69	Md	NCSN	
2001/03/22	12:31:54.10	40.1412	-123.2190	35.33	3.04	Md	NCSN	
2001/03/22	12:55:52.82	40.1240	-123.1968	35.22	3.02	Md	NCSN	
2001/03/22	21:22:30.11	40.3770	-126.5560	7.45	4.19	Md	NCSN	
2001/03/23	15:02:07.58	40.2437	-124.1607	12.75	3.33	Md	NCSN	
2001/03/27	12:21:49.84	40.4248	-124.3618	27.67	3.00	Md	NCSN	
2001/03/28	20:33:28.99	40.6202	-125.7368	6.22	3.21	Md	NCSN	
2001/04/20	05:19:51.86	40.6840	-125.3272	6.33	4.23	ML	NCSN	
2001/04/23	18:05:42.74	40.4187	-125.8607	5.00	3.33	Md	NCSN	
2001/04/28	03:54:22.86	39.5268	-123.0368	3.14	3.10	ML	NCSN	
2001/05/02	04:55:53.73	40.3270	-124.7000	14.75	4.09	ML	NCSN	
2001/05/03	10:49:19.88	40.4228	-125.0060	14.06	3.10	Md	NCSN	
2001/05/05	02:18:04.61	41.2253	-125.9150	4.98	3.01	Md	NCSN	
2001/05/22	00:40:39.39	40.4645	-124.8433	12.42	3.55	Md	NCSN	
2001/05/27	09:27:04.03	40.3750	-125.0195	0.31	3.14	Md	NCSN	

2001/06/07	23:38:14.00	40.6532	-124.6603	16.99	3.61	ML	NCSN	
2001/06/16	04:26:53.32	40.3030	-124.5298	20.98	3.36	Md	NCSN	
2001/07/12	06:10:33.91	41.2447	-123.5163	39.18	3.28	Md	NCSN	
2001/07/12	07:18:35.98	42.0712	-126.5167	5.14	3.66	Md	NCSN	
2001/07/15	06:56:53.44	40.4313	-126.8885	22.67	3.40	Md	NCSN	
2001/07/15	11:02:52.83	40.4158	-126.7735	4.23	3.39	Md	NCSN	
2001/07/31	20:21:36.11	40.3283	-124.6907	15.26	3.16	Md	NCSN	
2001/08/07	14:59:43.31	40.3490	-124.1773	30.97	3.14	Md	NCSN	
2001/08/26	20:41:24.92	40.3693	-124.9567	12.81	3.21	Md	NCSN	
2001/09/12	01:36:08.78	40.4032	-124.0882	21.73	3.00	Md	NCSN	
2001/09/12	01:39:10.89	40.3147	-124.6040	16.70	3.22	Md	NCSN	
2001/09/20	08:02:24.16	40.3718	-125.4173	26.81	4.66	Md	NCSN	
2001/10/10	23:49:37.88	40.3148	-125.8180	10.84	3.08	Md	NCSN	
2001/10/20	22:05:50.55	41.2667	-125.0500	5.01	3.12	Md	NCSN	
2001/10/22	08:23:51.71	40.9852	-124.2435	17.92	3.54	ML	NCSN	
2001/11/10	18:55:49.79	40.6820	-125.0302	4.98	3.36	Md	NCSN	
2001/11/18	02:17:00.01	41.2122	-125.8092	2.55	3.34	Md	NCSN	
2001/11/20	16:58:17.43	41.5682	-125.5560	5.19	3.10	Md	NCSN	
2001/11/21	02:01:28.99	41.7083	-126.0257	5.02	3.10	Md	NCSN	
2001/12/08	11:43:05.61	40.3912	-124.2335	14.70	3.17	Md	NCSN	
2001/12/10	09:09:27.17	40.5387	-125.9913	0.81	3.50	Md	NCSN	
2002/01/10	00:44:51.03	40.4420	-126.0720	23.72	3.80	Md	NCSN	
2002/01/12	21:52:50.92	41.2095	-124.2182	18.29	3.32	ML	NCSN	
2002/02/04	12:03:47.24	40.7858	-124.2992	22.66	3.16	ML	NCSN	
2002/02/08	18:38:46.20	40.7328	-126.1630	5.68	3.05	Md	NCSN	
2002/02/13	21:41:55.51	40.4417	-126.8582	12.94	3.57	Md	NCSN	
2002/03/18	20:37:11.53	40.4308	-126.3765	5.24	3.23	Md	NCSN	
2002/03/18	20:37:23.68	40.2848	-125.1632	0.06	3.06	Md	NCSN	
2002/03/27	03:53:04.92	40.2875	-125.2052	38.19	4.39	Md	NCSN	
2002/04/01	08:49:58.99	40.4105	-125.1117	0.08	3.71	Md	NCSN	
2002/04/10	16:38:12.61	40.6283	-125.0135	4.99	3.49	Md	NCSN	
2002/04/29	00:43:29.72	40.6007	-124.4555	29.77	4.36	ML	NCSN	
2002/05/04	04:58:52.13	40.2835	-124.4328	21.81	3.11	ML	NCSN	
2002/05/04	09:39:52.38	40.3177	-124.5338	4.92	3.04	Md	NCSN	
2002/05/04	10:20:23.60	40.3043	-124.4887	8.81	3.40	Md	NCSN	
2002/05/04	12:17:01.24	40.3032	-124.4847	8.49	3.70	Md	NCSN	
2002/05/04	12:54:24.91	40.3017	-124.4790	8.46	3.65	ML	NCSN	
2002/05/04	13:05:36.20	40.2998	-124.4613	9.23	3.60	Md	NCSN	
2002/05/04	13:28:08.61	40.3073	-124.4800	9.10	3.37	Md	NCSN	
2002/05/04	13:56:33.31	40.3085	-124.5185	7.74	4.26	ML	NCSN	
2002/05/04	14:24:48.42	40.3168	-124.4823	6.65	3.44	Md	NCSN	
2002/05/04	17:45:48.22	40.3122	-124.4528	8.00	3.44	ML	NCSN	
2002/05/04	19:33:00.34	40.3065	-124.4675	8.54	3.08	Md	NCSN	
2002/05/05	05:34:09.21	40.3152	-124.5588	6.80	3.30	Md	NCSN	
2002/05/06	07:43:24.00	40.3162	-124.4640	7.00	3.14	Md	NCSN	
2002/05/06	08:45:48.67	40.3080	-124.4735	7.64	3.27	ML	NCSN	
2002/05/08	14:28:42.35	40.4053	-125.2445	4.87	3.33	Md	NCSN	
2002/05/08	21:32:11.97	40.3310	-124.5275	0.67	3.19	ML	NCSN	
2002/05/09	05:56:35.76	40.3145	-124.4680	7.26	3.25	Md	NCSN	
2002/05/22	01:33:14.13	40.8152	-124.4293	23.33	3.69	ML	NCSN	
2002/05/29	19:30:09.39	40.1988	-124.1328	13.96	3.15	ML	NCSN	
2002/06/01	00:15:59.46	41.8845	-125.5813	2.51	3.65	Md	NCSN	
2002/06/11	04:30:55.41	40.3878	-125.0850	4.51	3.65	Md	NCSN	
2002/06/17	16:55:07.52	40.8228	-124.6020	22.34	5.09	ML	NCSN	*
2002/06/21	00:41:28.23	40.4520	-126.8093	11.58	3.23	Md	NCSN	
2002/06/30	02:51:41.54	40.4122	-126.8598	5.00	3.45	Md	NCSN	
2002/07/03	00:48:23.27	40.2790	-124.3835	15.06	3.32	ML	NCSN	
2002/07/03	12:58:57.40	39.4598	-123.3052	1.93	3.28	ML	NCSN	
2002/07/13	04:45:09.55	40.3982	-124.9340	16.42	3.09	Md	NCSN	
2002/07/14	03:52:34.33	41.2143	-126.1788	22.32	3.25	Md	NCSN	
2002/07/21	02:44:13.73	40.2998	-124.4803	13.23	3.29	Md	NCSN	
2002/07/30	19:03:22.13	41.7388	-125.8648	26.13	3.25	Md	NCSN	
2002/09/17	11:30:27.00	40.3623	-124.9647	1.92	3.02	Md	NCSN	
2002/10/17	08:12:01.64	40.4143	-126.4543	14.63	3.89	Md	NCSN	
2002/11/21	13:17:39.28	40.2973	-124.4148	8.92	3.59	Md	NCSN	
2002/11/24	22:46:56.63	39.9733	-124.0527	3.69	3.40	Md	NCSN	
2002/11/26	06:23:57.94	40.4265	-125.2625	7.25	3.00	Md	NCSN	
2002/12/23	04:16:03.72	40.3890	-124.1827	12.70	3.07	Md	NCSN	
2003/01/08	05:43:43.51	40.3822	-125.1383	2.61	4.07	Md	NCSN	
2003/01/14	15:51:33.24	40.7360	-124.5723	29.23	3.49	ML	NCSN	

2003/02/18	14:44:26.03	41.1172	-125.0235	2.54	3.63	Md	NCSN
2003/02/25	16:37:15.01	40.3963	-125.1960	0.31	3.51	Md	NCSN
2003/02/28	02:21:24.64	40.3985	-124.4232	30.99	3.24	Md	NCSN
2003/03/23	00:55:28.07	40.4800	-125.5993	4.95	3.06	Md	NCSN
2003/03/26	05:47:03.18	40.3907	-125.8873	5.08	3.00	Md	NCSN
2003/04/03	03:38:14.30	40.3183	-124.7767	14.89	3.36	Md	NCSN
2003/04/10	08:55:11.51	40.4388	-125.8768	11.40	3.13	Md	NCSN
2003/04/22	10:46:09.52	40.5848	-124.0762	28.55	3.91	ML	NCSN
2003/05/02	15:01:55.40	40.6467	-124.0367	26.10	3.12	Md	NCSN
2003/05/04	14:17:44.89	40.5460	-124.4225	33.68	3.17	Md	NCSN
2003/05/20	07:09:39.65	40.7645	-125.0220	13.53	3.09	Md	NCSN
2003/05/24	11:20:32.50	40.5080	-124.1913	19.46	3.15	ML	NCSN
2003/05/31	08:00:32.42	40.4815	-124.4387	26.54	3.05	ML	NCSN
2003/06/26	03:39:35.53	40.4193	-126.5083	3.42	3.75	Md	NCSN

[1]Magt: Magnitude type; Md: duration; ML: local; MB: body wave; Mlg: Lg

[2]SRC: Catalog Source; NCSN: Northern California Seismic Network; ISCCD: International Seismic Center CD; NEIC: National Earthquake Information Center.

CE: Calibration event

Task 2: Relocations

We have gathered all available phase data are in the process of formatting it for our use. We have yet to perform relocations, but plan to begin this effort by April 2004. Our approach will be to perform two distinct location algorithms. Each technique requires velocity models, and we have gathered models from previous work performed in the area. Figure 2 shows the velocity models by Oppenheimer et al. (1993), Henstock et al. (2003), and Verdonck and Zandt (1993). These models are also being used for our waveform modeling technique described below. We have begun calculating travel times for these models.

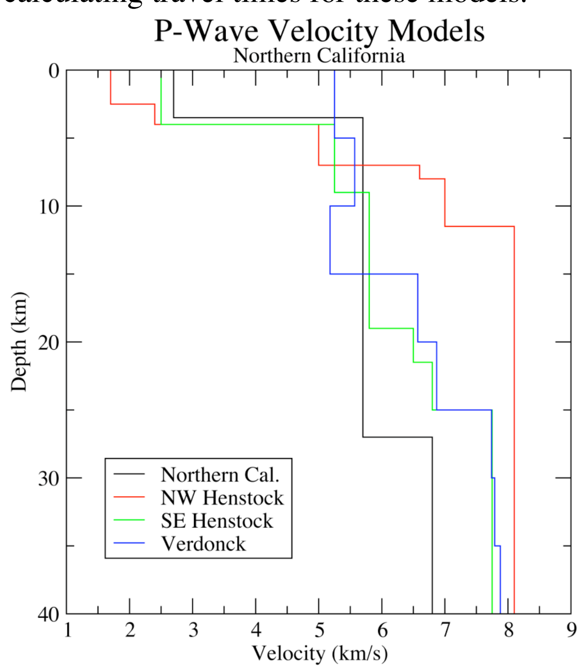

Figure 2: P-wave velocity models that will be used for our relocation effort. The models are also being used for our waveform modeling effort. Northern Cal is from Oppenheimer et al. (1993); NW and SE Henstock are the Northwest and Southwest models developed by Henstock et al. (2003), respectively; Verdonck is the model developed by Verdonck and Zandt (1994).

We will use an empirical calibration technique to obtain accurate locations for the MTJ region. This approach has been used to calibrate nuclear test sites in various countries around the world (e.g., Steck et al., 2001a). We will use travel time residuals of well-located events to construct correction surfaces, which will account for inadequate Earth models. The technique has proven to be useful for sparse networks, and may be effective to obtain accurate offshore event locations where station geometry is not optimal (Steck et al., 2001b). The correction surfaces will be constructed using the modified Bayesian kriging (MBK) method of Schultz et al (1998), which creates an interpolated surface from residuals using user-supplied correlation lengths of the background model and the data. MBK also produces an error variance surface associated with the correction surface, which allows for more realistic error ellipse estimation. Another location method that will be explored is the double-difference technique (Waldhauser and Ellsworth, 2000), which incorporates absolute travel-time measurements and/or cross-correlation *P*- and *S*- wave differential travel-time measurements. Observed and theoretical travel-time difference residuals are minimized using an iterative least squares solution. The technique has the advantage of minimizing velocity model errors without station corrections, similar to the MBK technique. Finally, a Joint Hypocenter Determination (JHD) approach may be applied which results in locations relative to a master event (Dewey, 1971, 1983). This technique has the ability to accurately locate events relative to one another, but may be off in an absolute sense if the master event is not accurately located. .

Task 3: Source parameter calibration and determination

We have made significant progress in modeling events in the region. We use a waveform inversion technique for smaller events, calculating synthetic Green's Functions assuming velocity models appropriate for the region. Results will then be used to interpret the state of stress for the region these events take place.

3.1 Models

We used four models for calculation of synthetic Green's Functions. Henstock and Levander (2003) developed a 2-D velocity model (Figure 2) using a seismic survey line from the 1994 MTJ Seismic Experiment (Mendocino Working Group, 1995). The velocity model of Henstock and Levander (2003) for line 3NWSE was used to construct two starting models (Figure 2). We estimated velocities at depths for the northwest and the southwest ends of the line. Another model was taken directly from Verdonck and Zandt's table (1994). Their model was created for the Mendocino area north and south of the triple junction using a large data set of events (1449 events) and a damped least squares inversion. A final model was from The North California Seismic Network Bulletin January - December 1992, (Oppenheimer, 1992) using the north California default model (Figure 2). Each of these models was used in the calculation of synthetic Greens functions for each of the five selected calibration events chosen.

The models used are all quite different from each other. The NorthCalDef model is the most simple with only four layers. The NWHenstock, SEHenstock, and Verdonck models all have many more layers than NorthCalDef. The models NorthCalDef, NWHenstock, and SEHenstock all have a similar layer at about 4km depth but have different velocities for it. Another similar layer occurs at 25km for all models (except NWHenstock), but again all have different velocities. There are no two models that are very similar to each other, each having a combination of features than are included in the others. However, we include analysis of all models with the hope that they may reveal specifically what model works best, which may depend on the location of the events.

3.2 Reflectivity Synthetic Greens Functions and Calibration Events

We calculate reflectivity Green's Functions using the method of Kennett (1993) applied by Randall et al. (1995). Four velocity models (described above) were used for all the possible stations that would be used in further analysis. We validate the velocity models by comparing results with five calibration events (described below). Calibration events were selected based on their higher magnitudes and locations along key portions of the seismic active zones within the region. They also required well-constrained Centroid Moment Tensor (CMT) solutions. Centroid Moment Tensors are a complete description of the size and source geometry of an earthquake. These calibration events were used to create synthetic Greens functions which were then compared to the data. The high magnitudes allowed a clear representation of the mechanism and the effect of the path of the event to the station where it was recorded. This made it easier to determine if a particular velocity model was a good approximation for that event path. The five events were selected in order to spread them out along the entire region where the smaller earthquakes seem to be clustered.

To test these models against the calibration events, we calculated synthetics using the Harvard Centroid Moment Tensor catalog. The recorded data for the events were then compared to synthetic Greens functions calculated for the same depth. Using various bandpasses on these synthetics and the calibration events for all stations, we compared the seismograms checking to make sure the synthetics approximated the calibration event data that was recorded at each station. When these models produced a good approximation, the models were used to calculate synthetic Greens functions for depths 1, 5, 10, 15, 20, 25, 30, and 35 kilometers for each of the calibrations events.

3.3 Time Domain Full Waveform Modeling

To invert for mechanism and depth, we use a regional time-domain waveform modeling technique (e.g. Langston, 1981). This technique involves a process where Green's functions for vertical strike-slip, vertical dip-slip, and 45°-dipping dip-slip (at 45° azimuth) are combined and inverted for fault planes and moment. The resulting combination for each radial, transverse, and vertical component was then compared to the data and evaluated for misfit. The rotated seismograms were used as data for the inversion codes. In this process the P-arrivals for each seismogram were picked and the data seismograms were decimated to match the synthetic reflectivity Greens functions calculated with the codes from Randall et al. (1995) for each of the velocity models. The output of the inversion code showed fits comparing the data using the inversion technique of Langston (1981) with the synthetics for depths of 1, 5, 10, 15, 20, 25, 30, and 35 kilometers for a given event.

The results indicated which focal depth was the best match for the selected velocity model. After a few iterations with unsuccessful results, we found that as the distance of an event from the calibration event increases new frequencies should be analyzed. At a distance of approximately 50km it appears that a bandpass of 100 seconds to 20 seconds was optimal. The synthetics and data for best fit would then be visually compared component by component to determine if the model matched the path from the event to that station. During the comparison, we noted that the shape of some data and synthetics would match, but would be shifted relative to each other, probably due to an error in event location. If the shift was less than 15 seconds the data were shifted in order to match the synthetic, this will correct for the event location errors. After visually comparing, removing, and shifting the data, the inversion was run again and would usually result in fits better than the unmodified data set.

We classified a good fit for data and synthetic to be one where the range of misfit values output would be consistent throughout the entire set of components for each station. Generally we considered a good fit to be below 0.65 for the misfit value. If the data and synthetic did not match the general form of each other (peaks and troughs), that component would be removed from the comparison. Data that matched the general form that also had large misfits were kept, except in the case that there was a large interference due to some other source that was not related to the event (noise). The focal mechanism associated with the event depth that provided the best fit was then used in the final analysis. This process was conducted for each event with each of the four velocity models developed.

3.4 Earth Simplification Transform

We have been successful in modeling smaller events using a suite of velocity models. However, smaller events will require shorter periods for modeling. Thus, we must develop other methods to obtain source parameters. We will use the calibration events (described above) to study the source parameters of the historic and smaller events in the region with the Earth simplification transform (EST) method developed by Zhang (1997). This method requires the calculation of synthetic waveforms and events with well-constrained mechanisms. With large events this technique can remove propagation effects so that the modeling of some smaller events may be performed for the region. We have prioritized the modeling on the larger magnitude events that have not already been modeled by either the Harvard Centroid Moment Tensor (Harvard CMT) or Berkeley Rapid Earthquake Data Integration (REDI) project and then to progress through to the smaller events.

This technique uses a deconvolution method, where the synthetic Greens function is deconvolved from the data of the large calibration event to provide a resulting difference between the two events. This difference is the propagation transfer function. It represents what one was unable to model using the synthetic Greens function. This propagation transfer function can then be deconvolved from a smaller event near the large calibration event. In effect this removes all the earth structure that could not be modeled in the synthetic Greens function from this small event, which leaves a simplified version of the small event's data, call the Earth Simplification Transform (EST) Seismogram. The EST Seismogram can then be used in an inversion to determine how closely it matches the original synthetic seismograms, which will result in estimates of depth and focal mechanism. The EST method is used for events that have a magnitude too small to be used in an inversion employing the synthetic Greens functions technique.

3.5 Results for waveform modeling

In order to obtain acceptable fits for each model, components that did not match well for the synthetic and observed data after all modifications were further analyzed and if determined the match was bad due to noise, they were removed. The largest factor that affected the inversions was noise. When using events of lower magnitudes, such as those in this study, noise can become overpowering. Good data with a high signal to noise ratio will result in much better fits with the synthetic seismograms and return more accurate moment tensors and moment release values.

After the modeling was complete, we compare the results from the different models. Of the ten modeled events (Figure 3), the Verdonck model produced the lowest mistfits for 4 events, NorthCalDef produced lowest misfits for 3 events, and SEHenstock produced lowest misfits for 3 events. In general, the best model was Verdonck, but the NorthCalDef, SEHenstock, and Verdonck models all were suitable models for this area. The events for each model with the lowest mistfit were plotted on a map to show the locations where the models were best (Figure 3).

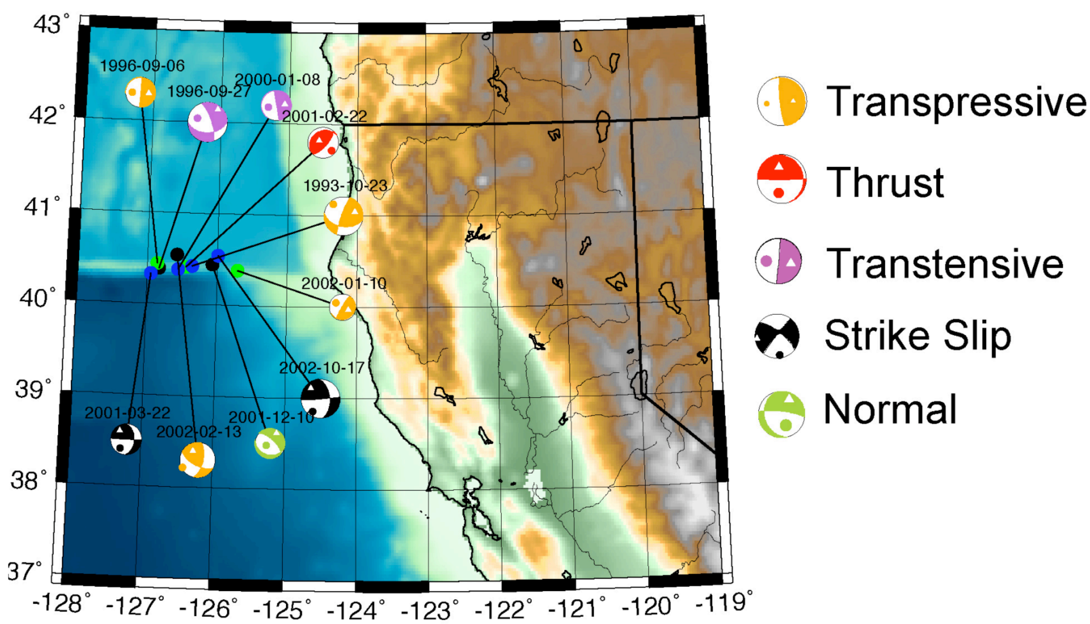

Figure 3: Map showing showing focal mechanisms for events modeled in this study along with velocity model associated with the best fitting solution for each focal mechanism. Black circles represent the NorthCalDef model, green circles represent the SEHenstock model, and blue circles represent the Verdonck model.

We find that we were successful in modeling $M_w < 4$ events without applying an EST. With the appropriate velocity model, we can obtain quality mechanisms and depths for these events. The threshold in which the EST may be most beneficial was not reached during the modeling performed in this study. The EST method is yet to be fully explored, and may play an important role in future work.

3.7 Stress Analysis

We use our modeled events (Table 3) plus the CMT solutions gathered from the NCEDC to map the stress axes in the region. We determine the P-axis and T-axis from the moment tensor solutions. We then classify all mechanism based on the P and T axes plunges into transpressive, thrust, transtensive, strike-slip, and normal events (Andronicos et al., 2004). We then sum of moment released for each event in the direction of the P-axis strike on a rose diagram; this will show the total amount of moment release against the azimuth it was released in. The rose diagram showing the total moment of all events shows that the P-axis (~σ1) of most moment release had a strike of 300 degrees to 330 degrees (Figure 4a). This orientation is consistent with moment release due to the Mendoncino fault.

We then separate the events into three categories, events of magnitude 3.0 to 4.5 (Figure 4b), 4.5 to 6.0 (Figure 4c), and 6.0 and above (Figure 4d). The results for the 3.0 to 4.5 and 4.5 to 6.0 rose diagrams were similar and resemble the rose diagram for all events. The rose diagram of 6.0 and above showed a completely different direction, with an average P-axis strike of 150 degrees to 180 degrees. There is virtually no moment release associated with a P-axis strike in the EW, the expected stress direction for the Cascadia subduction zone. The two most common directions being to the NW and to the S. The NW orientation seems to correlate with the stresses expected from the Mendocino Fracture Zone, and the South direction from the San Andreas Fault system.

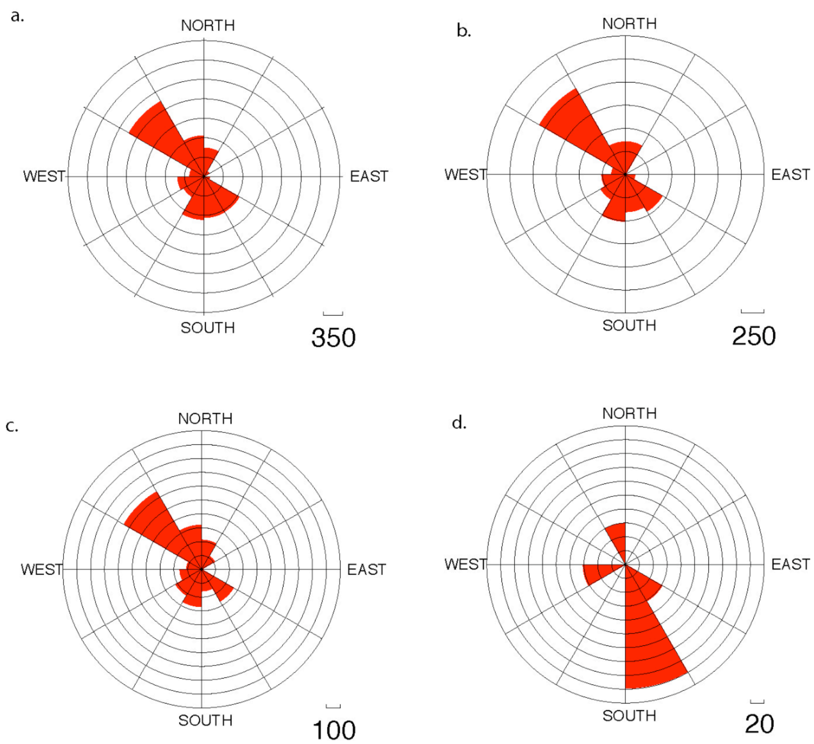

Figure 4: Rose diagrams plotting the log of sum of moment against the azimuth of the P-axis. (a.) All events, (b.) magnitude 3.0 - 4.5 (78 events), (c.) magnitude 4.5 - 6.0 (46 events), (d.) magnitude 6.0 and above (6 events).

We then sorted events by focal mechanism and made new rose diagram plots for normal/transtensive (Figure 5b), strike-slip (Figure 5c), and thrust/transpressive (Figure 5d). For the normal and transtensive events, there is no clear P-axis orientation. Upon closer investigation, E-W moment orientation is from one large event, the 1992-04-25 event with a moment release of $4.5x10^{26}$. Without this 1992-04-25 event, the trend is a definite N-S direction. Strike-slip events showed N-W oriented P-axis, and the thrust/transpressive showed an N-S oriented P-axis. The strike slip clearly following the pattern of release associated with the Mendocino fault and the thrust and transpressive events, excluding the 1992-04-25 event, also appear related to the San Andreas fault.

The largest events in the area are related to the San Andreas stress field orientation, and very little moment release is occurring in response to stresses related to the Cascadia Subduction Zone. This suggests that energy must be being stored for future large events or is currently being released a-seismically. Lack of seismic deformation is consistent with large events occurring on the Cascadia Subduction Zone once every 300-560 years (Clarke and Carver, 1992), with little seismic release in interim portion of the cycle. It is also observed that the events in the Gorda plate are mostly strike slip with a direction of N-NW (Stoddard, 1987; Wilson, 1989), consistent with the San Andreas stress field. This direction is not consistent with direction associated with the Cascadia Subduction Zone (E-W). This suggests that the dominant deformation of the Gorda plate is not caused by the Cascadia Subduction Zone, but instead the San Andreas fault system.

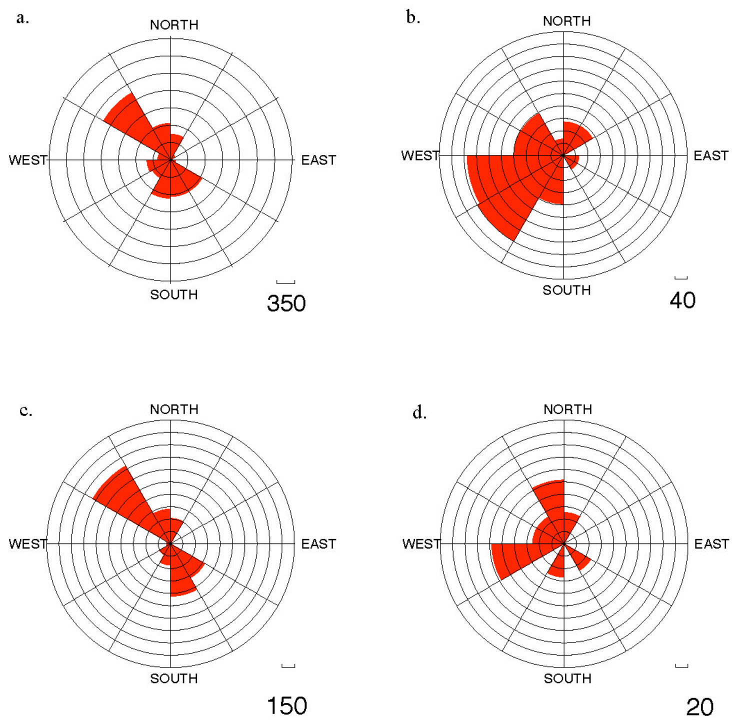

Figure 5: Rose diagrams plotting the log of sum of moment against the azimuth of the P-axis. (a.) All events (123 events), (b.) events classified as normal and transtensive (28 events), (c.) events classified as strike-slip (66 events), (d.) events classified as thrust and transpressive (10 events).

Task 4: Preliminary attenuation analysis

We have made significant progress on the attenuation analysis. During the first two weeks of September 2003, Dr. Roberto Ortega visited UTEP to assist in the process of the attenuation relations for the events listed in Table 2. Dr. Ortega, along with a graduate student, initiated the preprocessing of the ground motion scaling. Dr. Ortega visited UTEP again in January 2004, and has made some initial estimates. The work is ongoing.

Each seismogram was carefully reviewed, and we selected only well-located and high signal-to-noise ratio events for this analysis. In addition, the instrument response curves were carefully reviewed for accuracy. Each recording was organized in a hierarchical database, and we picked the *P* and *S* travel times of the vertical components and the entire earthquake record was corrected for the instrument response. The waveforms were filtered into 10 frequency bands using an 8-pole Butterworth filter with f_c frequencies equal to 0.2 0.4 0.7 1.0 2.0 3.0 4.0 5.0 6.0 and 7.0 Hz. The corner frequencies were given by 0.707 f_c and 1.41 f_c.. In addition, we computed the peak filter velocity and time duration between 5% and 75% of the integrated energy. This time duration is estimated starting from the *S* arrival and the integrated energy is normalized to a unit maximum value.

A spectral analysis was performed to obtain equivalent results such as those estimated for the time domain. The Fourier amplitude spectrum was computed and the root mean square (*RMS*) value between 0.707 f_c and 1.41 f_c was estimated. The time window used to estimate the Fourier transform is the same 5-75 % starting from the *S* arrival. The two values (maximum filtered velocity time series amplitude and the Fourier amplitude spectra *RMS* average over the frequency band between the cut-off frequencies) were stored in a table in addition to all statistical information. The waveform preprocessing is complete, and we are ready to estimate the attenuation relation, excitation and site terms using different techniques in the upcoming months.

References

Andronicos, C.L., Velasco, A.A., Hurtado, J.M., Crustal Deformation, in the India-Asia Collision Constrained by Earthquakes, *GSA Bulletin, accepted upon revision,* 2004.

Baker, M.R., and D.I. Doser, Joint inversion of regional and teleseismic waveforms, *J. Geophys. Res., 93*, 2037-2045, 1989.

Bakun, W., R., Seismicity of California's north coast, *Bull. Seismol. Soc. Am., 90*, 797-812, 2000.

Byerley, P., The earthquake of July 6, 1934, amplitudes and first motions, *Bull. Seism. Soc. Am., 28*, 1-14, 1938.

Clarke S. H. Jr. and Carver G. A., Late holocene tectonics and paleoseismicity, southern Cascadia subduction zone, *Science*, 255:188-192, 1992

Dengler, L., G. Carver, and R. McPherson, Sources of north coast seismicity, *Calif. Geol., 48*, 43-53, 1992.

Dewey, J. W., Seismicity studies with the method of joint hypocenter determination, *Ph.D. thesis*, 164 pp., University of California, Berkeley, 1971.

Dewey, J. W., Relocation of instrumentally recorded pre-1974 earthquakes in the South Carolina region, in Studies Related to the Charleston, South Carolina Earthquake of 1886, *U.S. Geol. Surv. Prof. Paper, 1313*, Q1-Q9, 1983.

Henstock, T.J., and A. Levander, Structure and seismotectonics of the Mendocino Triple Junction, California, J. Geophys. Res., 108(B5, 2260, doi:10.1029/2001JB000902, 2003.

Kennett, B.L.N, Seismic wave propagation in stratified media, Cambridge University Press, Cambridge, England, 342 pp., 1983.

Langston, C. A., Source inversion of seismic waveforms: the Koyna, India, Earthquakes of 13 September, 1967, *Bull. Seism. Soc. Am.*, 71, 1-24, 1981.

Oppenheimer, D., F. W. Klein, J. P. Eaton, F. W. Lester, The North California Seismic Network Bulletin, January - December 1992, Open-File Report - U. S. Geological Survey, Report: OF 93-0578, 45 pp., 1993.

Randall, George E., C.J. Ammon, and T.J. Owens, "Moment Tensor Estimation using Regional Seismograms from Portable Array Deployments", *Geophys. Res. Lett.*, 22, p1665-1668, 1995.

Schultz, C. A., S. C. Myers, J. Hipp, and C. J. Young, Nonstationary Bayesian kriging; a predictive technique to generate spatial corrections for seismic detection, location, and identification, *Bull. Seism. Soc. Am., 88*, 1275-1288, 1998.

Sparks, N.R., The Eureka earthquake of June 6, 1932, *Bull. Seismol. Soc. Am., 26*, 13-27, 1936.

Steck, L. K., A. A. Velasco, A. H. Cogbill, and H. J. Patton, Improving regional seismic event location in China, *Pure and Appl. Geophys.*, 158, 211-240, 2001.

Steck, L. K., M. L. Begnaud, and A. A. Velasco, On the use of kriged P-wave travel-time correction surfaces for seismic location, in *Proceedings of the 23rd seismic research review*, 410-419, 2001b.

Stoddard, P.R., A kinematic model for the evolution of the Gorda plate, *J. Geophys. Res.,* 92, 11524-11532, 1987.

Velasco, A.A., C.J. Ammon and T. Lay, Recent large earthquakes near Cape Mendocino and in the Gorda plate: broadband source time functions, fault orientations, and rupture complexities, *J. Geophys. Res., 99*, 711-728, 1994.

Verdonck, D. and Zandt, G., Three-Dimensional crustal structure of the Mendocino Triple Junction region and local earthquake travel times, Journal of Geophysical Research, v.99, 23843-23858, 1994

Waldhauser, F., and W. L. Ellsworth, A double-difference earthquake location algorithm: method and application to the northern Hayward fault, California, *Bull. Seism. Soc. Am.*, *90*, 1353-1368, 2000.

Wilson, D.S., A kinematic model for the Gorda deformation zone as a diffuse southern boundary of the Juan de Fuca plate, *J. Geophys. Res.*, 91, 10,259-10,269, 1986.

Wilson, D.S., Deformation of the so-called Gorda plate. *J. Geophys. Res.*, 94, 3065-3075, 1989.

Zhang, J., Source characterization using simplified waveforms: Tests on earthquakes and nuclear explosions in Xinjiang, China, *Bull. Seism. Soc. Am., 87*, 832846, 1997.

Non-technical Summary

The goal of our study is to better determine the locations, depths, source processes of historic and recent earthquakes, and develop preliminary attenuation models of the MTJ region. We wish to quantify the variability in energy release along important features in the MTJ region since 1906, relate the events to specific tectonic features, quantify differences in apparent stresses between intraplate and interplate events, and analyze attenuation and its impact on strong ground motion in the region. The bulk of our progress has been in data collection and we are moving toward analysis of the large amount of data that we have collected.

Reports Published

None at this time.

Data Availability Statement

We have gathered data from a variety of open sources, including the Northern California Seismic Center (NCSC), the United States Geologic Survey, the Incorporated Research Institutions for Seismology (IRIS), and various regional sources of information. We will be formatting this data into databases that may be useful to the community. Contact the lead PI for more information:

Aaron A. Velasco, University of Texas at El Paso, Geological Sciences, El Paso, TX 79968; Ph: (915) 747-5101; FAX (915) 747-5073; velasco@geo.utep.edu